IET Microwaves, Antennas & Propagation

Research Article

IET Journals
The Institution of Engineering and Technology

Wideband stacked maltese cross-shaped DR antenna for WiMAX and WLAN applications

ISSN 1751-8725
Received on 4th May 2016
Revised on 13th August 2016
Accepted on 31st August 2016
doi: 10.1049/iet-map.2016.0367
www.ietdl.org

Abhishek Sharma ✉, *Animesh Biswas*

Department of Electrical Engineering, IIT Kanpur, Kanpur 208 016, UP, India
✉ *E-mail: abhisheksharma.rf@gmail.com*

Abstract: A new maltese cross-shaped dielectric resonator (DR) antenna is presented and analysed as a wideband radiator. The antenna comprises of maltese cross-shaped DR, arranged in a stacked configuration and centrally fed by a coaxial probe. The proposed antenna radiates such as an electric monopole, generating omnidirectional linearly polarised fields. Three modes: namely, $TM_{01\delta}$, $TM_{02\delta}$, and $TM_{03\delta}$ are simultaneously excited and merged in the composite structure to obtain a wide bandwidth of 59.5% [for voltage standing wave ratio≤2], covering frequency range from 3.15 to 5.82 GHz. The radiation pattern of the proposed antenna is fairly stable throughout the operating band with the measured peak gain varies from 3.27 to 6.09 dBi. A prototype of the proposed antenna is built and tested. Both the simulations and experimental results are presented and discussed. The proposed antenna is suitable candidate for worldwide interoperability for microwave access (3.5 GHz) and wireless local area network (3.65 GHz/4.9 GHz/5 GHz) applications. Moreover, it can also be used for lower European ultra-wideband frequency band (3.4–5 GHz) applications.

1 Introduction

Dielectric resonator antennas (DRAs) have been investigated extensively over the past few decades since their inception in 1983 by Long *et. al.* [1]. Unlike conventional microstrip antennas, DRA offers several advantages such as compact size, low loss, wide bandwidth, minimal conductor loss, absence of surface waves [2] etc. In 1989, Kishk *et al.* [3] have experimentally studied the broadband DRA for the first time, where the two DRAs were stacked over one another to get the broadband characteristics. Since then, a considerable amount of research on DRA has been focused on exploring the techniques for bandwidth enhancement. Various methods which include stacking [4–6], mode merging [7, 8], composite, and hybrid structures [9–12], conformal feed DRAs [13, 14] have been reported in the past. However, the DRA under investigation in the above referred designs radiates in broadside direction.

The cylindrical DR fed centrally by a coaxial probe generates transverse magnetic $(TM)_{01\delta}$ mode which results in omnidirectional radiation. To the best of our knowledge, a handful of wideband designs having omnidirectional radiation pattern were reported. For instance, two variants of stacked annular ring [15, 16] have been proposed for wideband operation. An impedance bandwidth of 45% has been achieved using disc-ring DRA antenna *in* [17]. In an another work [18], a truncated annular conical DRA with wide bandwidth and monopole-type pattern has been investigated for body area network applications. In [19, 20], four cylindrical DR were arranged in circular fashion and each element was excited in hybrid mode $(HE)_{11\delta}$ mode and composite field patterns result in wideband monopole-type radiation. A half hemispherical DRA [21] and a segmented DRA [22] having impedance bandwidth of 35 and 30%, respectively, have been reported for broadband monopole-type radiation. A wideband annular column loaded cylindrical DRA having conical radiation has been proposed in [23]. Zou and Pan [24] have investigated resonant modes in a wideband hybrid omnidirectional rectangular DRA and showed that the omnidirectional mode of the rectangular DR is a combination of the higher-order transverse electric $(TE)^{x}_{121}$ and TE^{y}_{211} modes. Some ultra-wideband (UWB) DRAs having omnidirectional radiation have also been investigated [25–27]. However, these designs are high profile in nature.

In this paper, a novel shape of DR is conceived through geometrical modifications of cylindrical DR which is investigated as a non-conventional shape that will generate omnidirectional radiation over the wide bandwidth. In the proposed design, mode merging technique is exploited where three resonant modes ($TM_{01\delta}$, $TM_{02\delta}$, and $TM_{03\delta}$) are simultaneously excited in the composite structure to achieve wide continuous bandwidth. All these modes are radiating in similar manner such as short electric monopole. The initial design parameters are determined using analytical formula and then subsequently optimised through simulations using Ansoft high-frequency structure simulator which is based on finite element method.

2 Antenna configuration and design

The geometry of the proposed antenna is schematically shown in Fig. 1. It constitutes two maltese-shaped DR of different dimension stacked over one another. The lower DR has the dimensions: radius R_l and height h_l and the upper DR has the dimensions: radius R_u and height h_u. The antenna rests on a square metallic ground plane of length $L = 130$ mm and thickness $t = 1$ mm. A coaxial probe of length p_h (above the ground plane) is introduced at the centre to excite the antenna. The antenna is designed in four stages as depicted in Fig. 2 to realise wideband characteristics. The steps are as follows: (a) a cylindrical DRA with $\varepsilon_r = 10.2$ is designed at 3.6 GHz and is referred as Ant 1. (b) Ant 2 is designed by stacking larger cylindrical DR of same permittivity over the smaller DR. (c) To realise the Ant 3, the cylindrical geometry is perturbed such that it transforms into the maltese cross shape. (d) Furthermore, four circular holes of radius R_s (see Fig. 1*b*) are made in lower DR of Ant 3 to realise the proposed antenna.

2.1 Design analysis

Fig. 3 shows the simulated voltage standing wave ratio (VSWR) and input impedance response of the reference antennas and the proposed antenna. From this figure, it is observed that two adjacent resonances exist in Ant 1 which is excited centrally by a coaxial probe. The

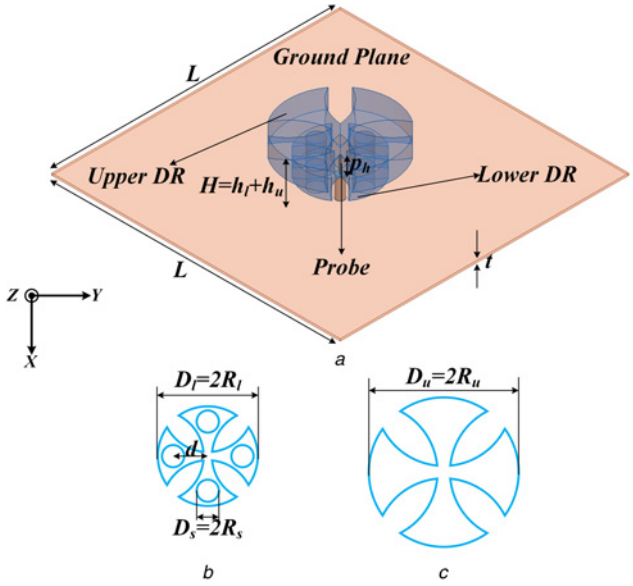

Fig. 1 *Geometry of the proposed antenna*

a Isometric view
b Lower DR
c Upper DR

lowest-order mode is $TM_{01\delta}$ and its resonant frequency can be determined by [2]

$$f_r(TM_{01\delta}) = \frac{4.7713\sqrt{\mathbf{14.66} + \left((\pi a/2h)\right)^2}}{a\sqrt{\epsilon_r + 2}} \quad (1)$$

where $\boldsymbol{a}$, $\boldsymbol{h}$, and ϵ_r are the radius, height, and relative permittivity of cylindrical DR, respectively. The theoretical resonant frequency of fundamental $TM_{01\delta}$ mode is 3.6 GHz and match well with the simulated value (3.58 GHz, indicated by the first peak of the real part of input impedance curve after de-embedding the port). The magnetic field distribution in Ant 1 at two different frequencies is shown in Fig. 4*a*, which confirms the excitation of fundamental $TM_{01\delta}$ mode at 3.58 GHz and next higher-order $TM_{02\delta}$ mode at 5.30 GHz.

When a cylindrical DR of radius $R_u > R_l$ is placed on the top of lower DR (see Fig. 2*b*), the previously existed resonances at 3.58 and 5.30 GHz are now shifted to 3.34 and 4.21 GHz due to the loading effect of the larger DR. Additionally, an extra resonance becomes notable at 5.04 GHz. It is evident from Fig. 3 that, *the*

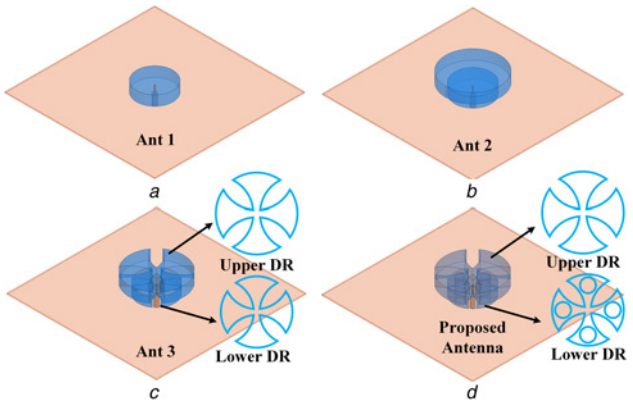

Fig. 2 *Geometry of reference and proposed antennas*

a Cylindrical DRA (Ant 1)
b Stacked cylindrical DRA (Ant 2)
c Stacked maltese cross-shaped DRA (Ant 3)
d Proposed antenna

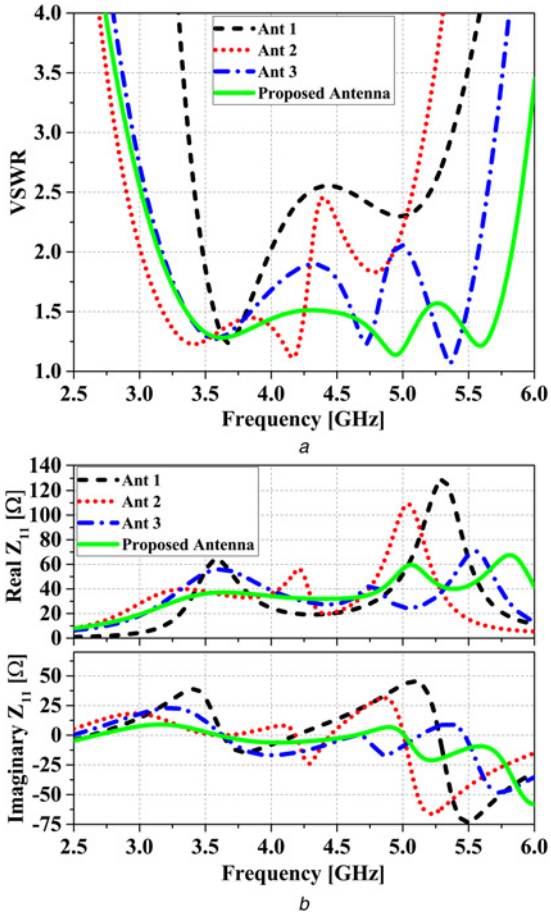

Fig. 3 *Simulated response of reference antennas and the proposed antenna*

a VSWR
b Input impedance

good matching in lower frequency band results in wider bandwidth as compared with Ant 1. The magnetic field distribution in Ant 2 at three different resonant frequencies corresponding to $TM_{01\delta}$, $TM_{02\delta}$, and $TM_{03\delta}$ modes are illustrated in Fig. 4*b*.

To further improve the performance, the geometry is perturbed by removing some portion from both the cylindrical DR which transform the geometry into maltese cross shape. The perturbation lowers the effective permittivity which in turn reduces the Q-factor ($Q \propto \epsilon_{\text{eff}}^{P}$, $P > 1$ [2]) and enhances the antenna bandwidth. Owing to the decrease in the value of effective permittivity, the resonant frequency of all three modes shifts upwards from 3.34, 4.21, and 5.04 GHz to 3.61, 4.76, and 5.55 GHz as shown in Fig. 3*b*. Though, the bandwidth of Ant 3 is wider than Ant 2 but the higher side of frequency band is still not matched which result in discontinuous bandwidth as depicted in Fig. 3*a*.

Finally, to further enhance the bandwidth, circular holes of radius R_s are introduced in the lower DR. The perforations (circular holes) in the DR further reduces the quality factor by lowering down the effective permittivity as well as match the higher side of frequency band, leading to wide bandwidth of 59.6% (for VSWR ≤ 2), covering the frequency range from 3.15 to 5.83 GHz. Alike the previous case, here also the resonant frequency of all the modes increases from 3.61, 4.76, and 5.55 GHz to 3.625, 5.06, and 5.81 GHz because of reduction in effective permittivity. Figs. 4*c* and *d* depict the magnetic field distribution in Ant 3 and proposed antenna, respectively.

3 Parametric analysis

The judicious selection of size and position of perforations (circular holes) should be made in order to get the broad bandwidth. In this section, parametric analysis is carried out to scrutinise the effect of

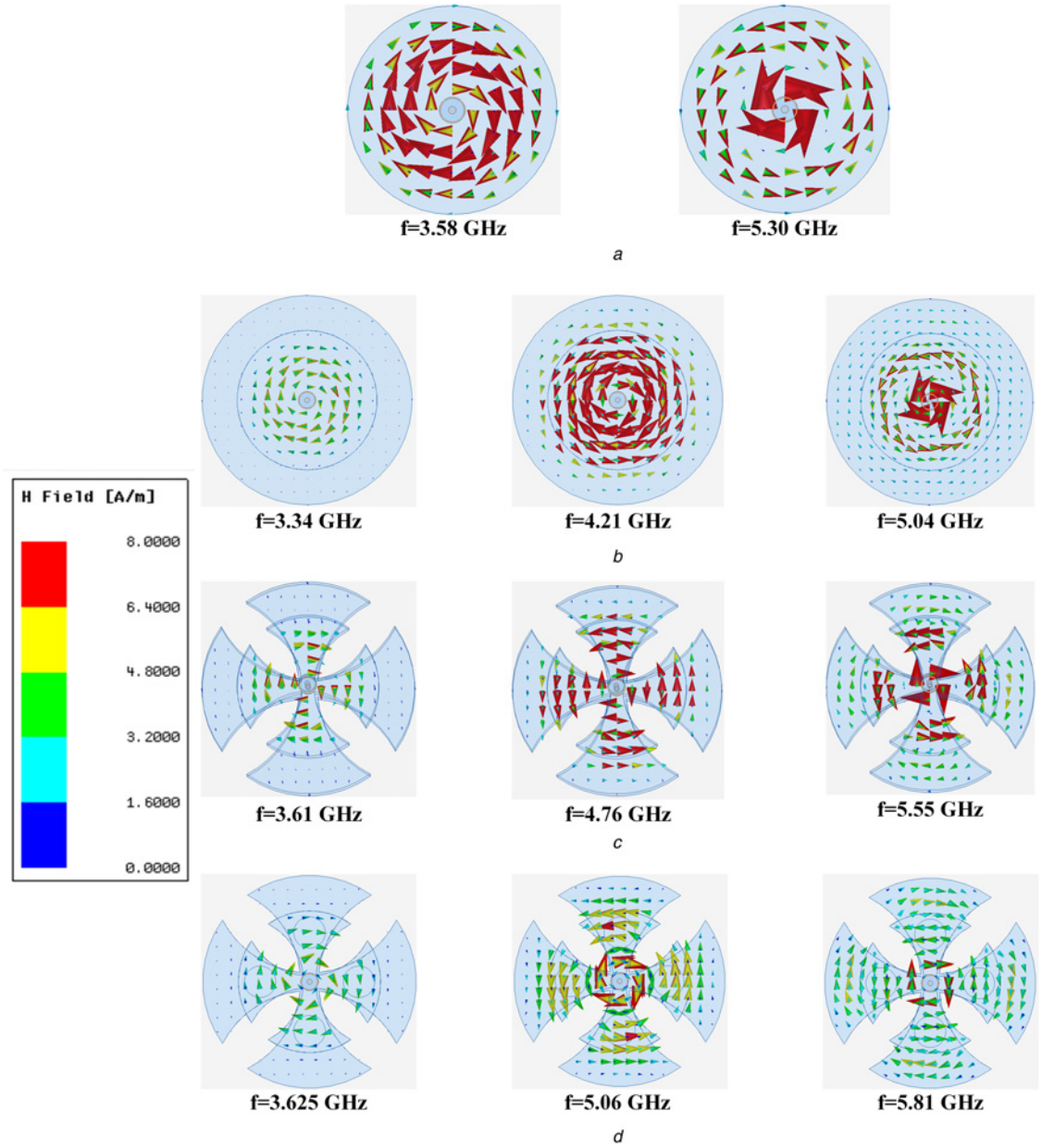

Fig. 4 *Magnetic field distribution of*
a Ant 1
b Ant 2
c Ant 3
d Proposed antenna

circular hole position and size. Moreover, the effect of probe height p_h and radius of upper DR R_u are also critically examined.

3.1 Effect of circular hole position (d)

Fig. 5 shows the simulated VSWR for different values of d keeping the other parameters constant. It is observed that as d increases from 10.5 to 13.5 mm, the matching becomes better in the desired frequency range. For $d = 13.5$ mm, the circular holes touch the periphery of DR and makes the fabrication difficult. Therefore, for the present paper the value of d is chosen as 12.5 mm.

3.2 Effect of circular hole radius (R_s)

The simulated VSWR for different values of R_S keeping the other parameters constant is presented in Fig. 6. On increasing the radius of circular hole, the effective permittivity decreases which in turn reduces Q-factor leading to wide bandwidth. Though the bandwidth is wider for the case when $R_s = 5$ mm but for this value the circular hole touches the periphery of the DR which makes the fabrication burdensome. Thus, the value of radius is chosen as 4 mm.

3.3 Effect of probe height (p_h)

In Fig. 7, the simulated VSWR of the proposed antenna with different probe length p_h is presented and pronounce effect of p_h is revealed. It is found that the better matching occurs in the desired frequency band when the probe length is 8 mm above the ground plane.

3.4 Effect of upper DR radius (R_u)

Fig. 8 depicts the effect of different values of R_u on the VSWR of the proposed antenna keeping the other dimensions constant. It is evident from this figure that on increasing the value of R_u from

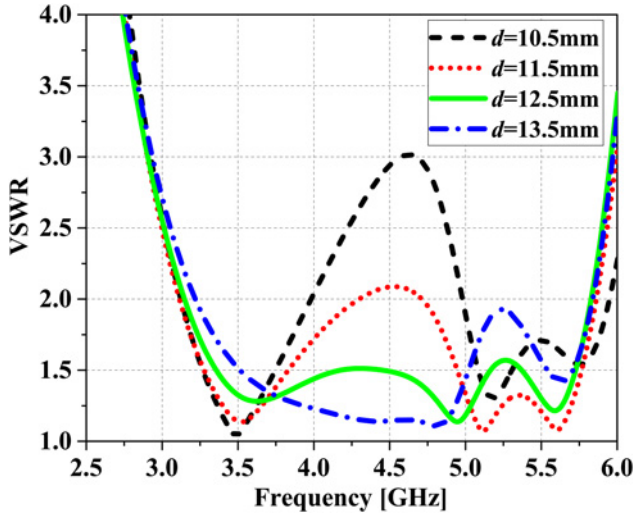

Fig. 5 *Simulated VSWR response of the proposed antenna for different values of d (R_l = 18 mm, R_u = 27 mm, h_l = 10 mm, h_u = 10 mm, R_s = 4 mm, and p_h = 8 mm)*

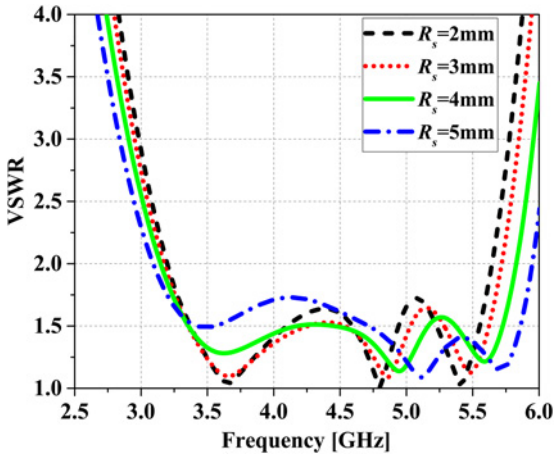

Fig. 6 *Simulated VSWR response of the proposed antenna for different values of circular hole radius R_s (R_l = 18 mm, R_u = 27 mm, h_l = 10 mm, h_u = 10 mm, d = 12.5 mm, and p_h = 8 mm)*

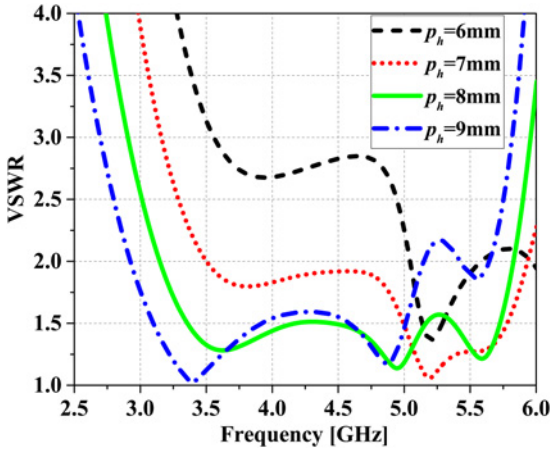

Fig. 7 *Simulated VSWR response of the proposed antenna for different probe length p_h (R_l = 18 mm, R_u = 27 mm, h_l = 10 mm, h_u = 10 mm, R_s = 4 mm, and d = 12.5 mm)*

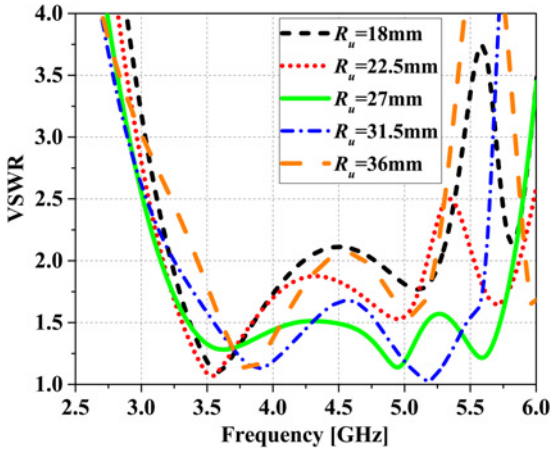

Fig. 8 *Simulated VSWR response of the proposed antenna for different values of R_u (R_l = 18 mm h_l = 10 mm, h_u = 10 mm, R_s = 4 mm, d = 12.5 mm, and p_h = 8 mm)*

$R_u = R_l = 18$ mm to $R_u = 1.5\ R_l = 27$ mm, the bandwidth increases. After that bandwidth reduces and VSWR curve becomes worst. Thus, for the best bandwidth R_u is chosen as 27 mm.

4 Results and discussion

A prototype of the proposed antenna is fabricated out from Rogers RT/Duroid 6010 of relative permittivity 10.2 and loss tangent 0.0023 for experimental verification. The optimised dimensions of the antenna are: R_l = 18 mm, R_u = 27 mm, h_l = 10 mm, h_u = 10 mm, R_s = 4 mm, d = 12.5 mm, and p_h = 8 mm.

The measured and simulated VSWR of the proposed antenna is shown in Fig. 9. The measured bandwidth of antenna is 59.5% (3.15–5.82 GHz) and agrees with the simulated bandwidth which is 59.6% (3.15–5.83 GHz).

Fig. 10 shows the simulated and measured normalised radiation pattern in the H-plane (xy-plane) and E-plane (xz-plane) of the proposed antenna at three different frequencies within the band of interest. It is observed that radiation pattern is quite stable over the entire spectrum. Both simulated and measured cross-polar level is below −10 dB in the H-plane. In the E-plane, the simulated and measured cross-polar level is below −30 and −20 dB, respectively. The peak gain variation of antenna is depicted in Fig. 11. The simulated peak gain of antenna varies from 3.90 to 6.17 dBi, whereas the measured peak gain ranges from 3.27 to 6.09 dBi. Some discrepancy in the DRA measurement is not unusual which is owing to fabrication tolerances and inevitable air gap that exist

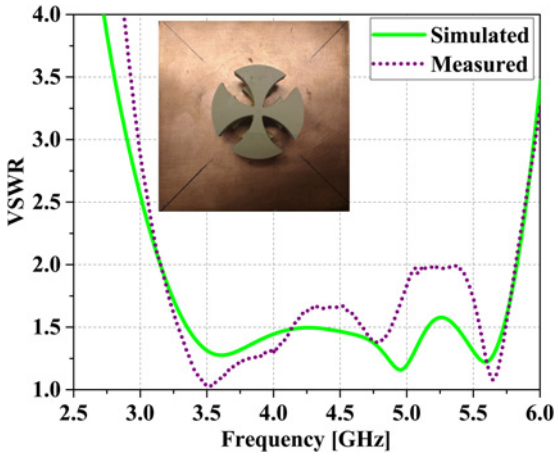

Fig. 9 *Simulated and measured VSWR response of the proposed antenna*

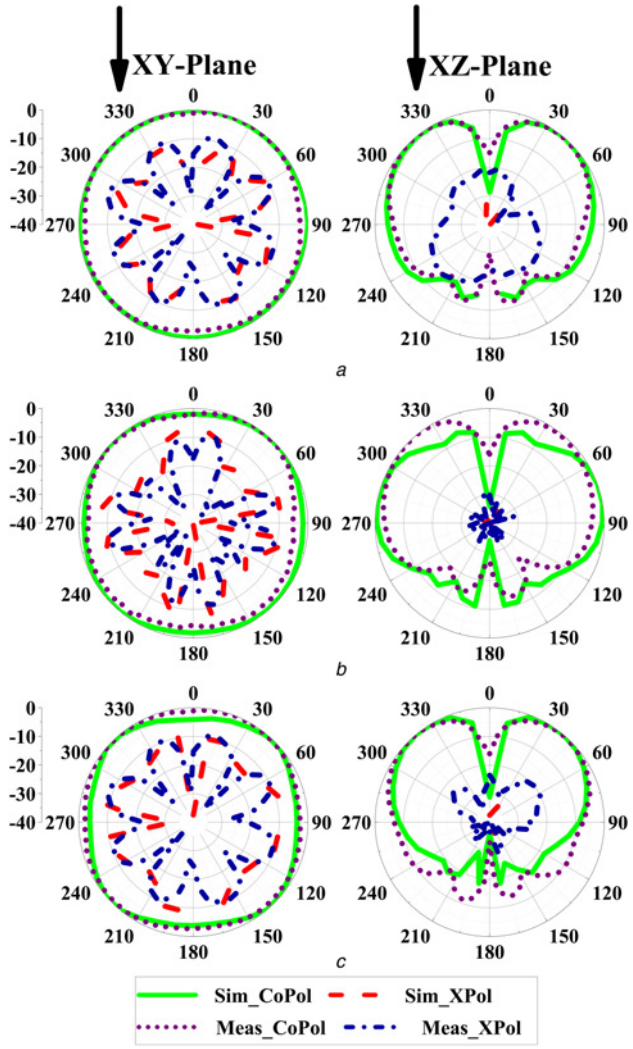

Fig. 10 *Normalised radiation pattern in H-plane (XY-plane) and E-plane (XZ-plane) at*

a 3.62 GHz
b 5.00 GHz
c 5.60 GHz

between the DRA and the metallic ground plane. The adhesive that is used to glue the DR with ground plane might affect the performance as well.

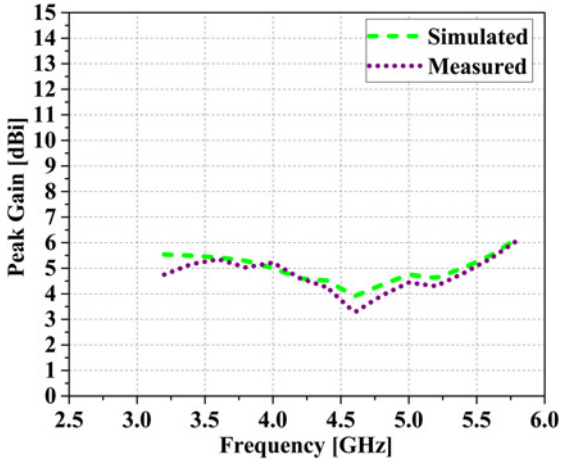

Fig. 11 *Simulated and measured peak gain variations of the proposed antenna*

Table 1 Comparison of different wideband DRAs

DRA references	Modes	BW, %	**Peak** gain, dBi
[15]	$TM_{01\delta}$	18 (5–6 GHz)	NA
[16]	$TM_{01\delta}$	42 (3.6–5.5 GHz)	5.5
[17]	$TM_{01\delta}$	45 (2.2–3.5 GHz)	NA
[18]	$TM_{01\delta}$	50 (3–5 GHz)	NA
[19]	$HEM_{11\delta}$	29 (3–4 GHz)	4
[20]	$HEM_{11\delta}$	49 (3.48–5.82 GHz)	4–6
[21]	$HEM_{11\delta}$, TM_{101}	35 (2.8–4 GHz)	5
[22]	$HEM_{11\delta}$, TM_{101}	26 (2.7–3.5 GHz)	NA
[23]	$TM_{01\delta}$, $TM_{02\delta}$, $TM_{03\delta}$, $TM_{04\delta}$	56 (3.14–5.56 GHz)	3–8.7
proposed antenna	$TM_{01\delta}$, $TM_{02\delta}$, $TM_{03\delta}$	**59.5 (3.15–5.82 GHz)**	**3.27–6.09**

BW: Bandwidth

A comparison of the proposed antenna with some previously reported literature is given in Table 1.

5 Conclusion

A stacked maltese cross-shaped DRA for wideband applications has been proposed. Three modes ($TM_{01\delta}$, $TM_{02\delta}$, and $TM_{03\delta}$) are simultaneously excited and merged in the composite structure to obtain a wide bandwidth with omnidirectional radiation pattern. Experimental results show that the proposed antenna exhibits impedance bandwidth of 59.5%, covering the frequency range from 3.15 to 5.82 GHz. The radiation pattern of the antenna is fairly stable throughout the band with the measured cross-polar level below −10 dB in H-plane and −20 dB in E-plane. The peak gain of the proposed antenna varies from 3.27 to 6.09 dBi in the passband. The proposed antenna could be a good candidate for worldwide interoperability for microwave access (3.5 GHz) and wireless local area network (3.65 GHz/4.9 GHz/5 GHz) band applications. Additionally, it could be suitable for lower European UWB frequency band (3.4–5 GHz) applications.

6 References

1 Long, S.A., McAllister, M., Liang, S.: 'The resonant cylindrical dielectric cavity antenna', *IEEE Trans. Antennas Propag.*, 1983, **31**, (3), pp. 406–412
2 Mongia, R.K., Bhartia, P.: 'Dielectric resonator antennas – a review and general design relations for resonant frequency and bandwidth', *Int. J. RF Microw. Comput.-Aided Eng.*, 1994, **4**, (3), pp. 230–247
3 Kishk, A.A., Ahn, B., Kajfez, D.: 'Broadband stacked dielectric resonator antennas', *IET Electron. Lett.*, 1989, **25**, (18), pp. 1232–1233
4 Kishk, A.A., Zhang, X., Glisson, A.W., *et al.*: 'Numerical analysis of stacked dielectric resonator antenna excited by a coaxial probe for wideband applications', *IEEE Trans. Antennas Propag.*, 2003, **51**, (8), pp. 1996–2006
5 Huang, W., Kishk, A.A.: 'Compact wideband multi-layer cylindrical dielectric resonator antenna', *IET Microw. Antennas Propag.*, 2007, **1**, (5), pp. 998–1005
6 Walsh, A.G., Young, C.S.D., Long, S.A.: 'An investigation of stacked and embedded cylindrical dielectric resonator antennas', *IEEE Antennas Wirel. Propag. Lett.*, 2006, **5**, pp. 130–133
7 Chang, T.H., Kiang, J.F.: 'Bandwidth broadening of dielectric resonator antenna by merging adjacent bands', *IEEE Trans. Antennas Propag.*, 2009, **57**, (10), pp. 3316–3320
8 Rashidian, A., Shafai, L., Klymyshyn, D.M.: 'Compact wideband multimode dielectric resonator antennas fed with parallel standing strips', *IEEE Trans. Antennas Propag.*, 2012, **60**, (11), pp. 5021–5031
9 Chair, R., Kishk, A.A., Lee, K.F.: 'Wideband stair-shaped dielectric resonator antennas', *IET Microw. Antennas Propag.*, 2007, **1**, (2), pp. 299–305
10 Esselle, K.P., Bird, T.S.: 'A hybrid resonator antenna: experimental results', *IEEE Trans. Antennas Propag.*, 2005, **52**, (2), pp. 870–871
11 Kishk, A.A., Yin, Y., Glisson, A.W.: 'Conical dielectric resonator antennas for wide-band applications', *IEEE Trans. Antennas Propag.*, 2002, **50**, (4), pp. 469–474
12 Chair, R., Kishk, A.A., Lee, K.F.: 'Low profile wideband embedded dielectric resonator', *IET Microw. Antennas Propag.*, 2007, **1**, (2), pp. 294–298
13 Chu, L.C.Y., Guha, D., Antar, Y.M.M.: 'Conformal strip-fed shaped cylindrical dielectric resonator: Improved design of a wideband wireless antenna', *IEEE Antennas Wirel. Propag. Lett.*, 2009, **8**, pp. 482–485

14 Liang, X.L., Denidni, T.A., Zhang, L.N.: 'Wideband L-shaped dielectric resonator antenna with conformal inverted trapezoidal patch feed', *IEEE Trans. Antennas Propag.*, 2009, **57**, (1), pp. 271–274
15 Shum, S.M., Luk, K.M.: 'Stacked annular ring dielectric resonator antenna excited by a axi-symmetric coaxial probe', *IEEE Trans. Antennas Propag.*, 1995, **43**, (8), pp. 889–892
16 Guo, Y.X., Ruan, Y.F., Shi, X.Q.: 'Wideband stacked double annular ring dielectric resonator antenna at the end-fire mode operation', *IEEE Trans. Antennas Propag.*, 2005, **53**, (10), pp. 3394–3397
17 Ong, S.H., Kishk, A.A., Glisson, A.W.: 'Wideband disk-ring dielectric resonator antenna', *Microw. Opt. Technol. Lett.*, 2002, **35**, (6), pp. 425–428
18 Almpanis, G., Fumeaux, C., Frohlich, J., *et al.*: 'A truncated conical dielectric resonator antenna for body-area network applications', *IEEE Antennas Wirel. Propag. Lett.*, 2009, **8**, pp. 279–282
19 Guha, D., Antar, Y.M.M.: 'Four element cylindrical dielectric resonator antenna for wideband monopole-like radiation', *IEEE Trans. Antennas Propag.*, 2006, **54**, (9), pp. 2657–2662
20 Choudhary, R.K., Srivastava, K.V., Biswas, A.: 'Broadband four-element multi-layer multi-permittivity cylindrical dielectric resonator antenna', *Microw. Opt. Technol. Lett.*, 2013, **55**, (5), pp. 932–937
21 Guha, D., Antar, Y.M.M.: 'New half-hemispherical dielectric resonator antenna for broadband monopole-type radiation', *IEEE Trans. Antennas Propag.*, 2006, **54**, (12), pp. 3621–3628
22 Guha, D., Gupta, B., Kumar, C., *et al.*: 'Segmented hemispherical DRA: new geometry characterized and investigated in multi-element composite forms for wideband antenna applications', *IEEE Trans. Antennas Propag.*, 2012, **60**, (3), pp. 1605–1610
23 He, Y., Lin, Y., Deng, C., *et al.*: 'Annular column loaded cylindrical dielectric resonator antenna for wideband conical radiation', *IEEE Trans. Antennas Propag.*, 2015, **63**, (12), pp. 5874–5878
24 Zou, M., Pan, J.: 'Investigation of resonant modes in wideband hybrid omnidirectional rectangular dielectric resonator antenna', *IEEE Trans. Antennas Propag.*, 2015, **63**, (7), pp. 3272–3275
25 Lapierre, M., Antar, Y.M.M., Ittipiboon, A., *et al.*: 'Ultra wideband monopole/dielectric resonator antenna', *IEEE Microw. Wirel. Compon. Lett.*, 2005, **15**, (1), pp. 7–9
26 Ghosh, S., Chakrabarty, A.: 'Ultrawideband performance of dielectric loaded T-shaped monopole transmit and receive antenna/EMI sensor', *IEEE Antennas Wirel. Propag. Lett.*, 2008, **7**, pp. 358–361
27 Guha, D., Gupta, B., Antar, Y.M.M.: 'Hybrid monopole-DRAs using hemispherical/conical-shaped dielectric ring resonators: improved ultrawideband designs', *IEEE Trans. Antennas Propag.*, 2012, **60**, (1), pp. 393–398